REFERENCES AND NOTES

1. B. Bass, in *The RNA World*, R. F. Gesteland and J. F. Atkins, Eds. (Cold Spring Harbor Laboratory Press, Cold Spring Harbor, NY, 1993), chap. 15.
2. B. Sommer, M. Kohler, R. Sprengel, P. H. Seeburg, *Cell* **67**, 11 (1991); H. Lomeli et al., *Science* **266**, 1709 (1994); M. Kohler, N. Burnashev, B. Sakmann, P. Seeburg, *Neuron* **10**, 491 (1993); J. Egebjerg and S. F. Heinemann, *Proc. Natl. Acad. Sci. U.S.A.* **90**, 755 (1993).
3. N. Nakanishi, N. A. Shneider, R. Axel, *Toxicon* **28**, 1333 (1990); K. Keinänen *et al.*, *Science* **249**, 556 (1990); J. Boulter *et al.*, *Neuron* **3**, 589 (1989); K. Sakimura *et al.*, *FEBS Lett.* **272**, 73 (1990).
4. R. I. Hume, R. Dingledine, S. F. Heinemann, *Science* **253**, 1028 (1991); R. Dingledine, R. Hume, S. Heinemann, *J. Neurosci.* **12**, 4080 (1992); T. Verdoorn, N. Burnashev, H. Monyer, P. Seeburg, B. Sakmann, *Science* **252**, 1715 (1991); M. Mishina *et al.*, *Biochem. Biophys. Res. Commun.* **180**, 813 (1991).
5. M. Higuchi *et al.*, *Cell* **75**, 1361 (1993); J. Egebjerg, V. Kukekov, S. F. Heinemann, *Proc. Natl. Acad. Sci. U.S.A.* **91**, 10270 (1994).
6. We established permanently transfected polyclonal cell lines by using calcium phosphate coprecipitation with a eukaryotic expression vector (pRC/CMV; Invitrogen) containing a 5-kb (2-exon) or 646–base pair (bp) GluR-B transcription unit. Total RNA was prepared by the guanidinium isothiocyanate method (7). Total RNA (2.5 μg) was reverse transcribed with an intronic antisense primer (+390 to +407 relative to the Q/R site); PCR amplification of cDNA was achieved with the initial cDNA synthesis primer and an expression vector–specific primer (5′-CTGGCTTATCGAAATTAATACGAC-3′). The product was purified on a 0.8 or 2% agarose gel and 2 pmol was annealed to a γ-^{32}P–labeled 17-nt oligomer antisense primer corresponding to positions +3 to +19. The primer was extended in the presence of 40 mM tris-HCl (pH 7.5), 50 mM NaCl, 20 mM $MgCl_2$, 3.6 mM $MnCl_2$, 200 μM each of deoxyadenosine 5′-triphosphate, deoxyguanosine 5′-triphosphate, and deoxycytidine 5′-triphosphate, and 1200 μM dideoxythymidine 5′-triphosphate by using 1.6 U of Sequenase (United States Biochemicals) for 10 min at 37°C. Primers annealed to nonedited and edited sequences were extended to the first or second upstream A, generating products of 20 and 24 nt, respectively; the resulting products were separated on a 20% acrylamide–7 M urea gel. Editing was quantified with a Molecular Dynamics phosphorimager.
7. F. Ausubel *et al.*, Eds., *Current Protocols in Molecular Biology* (Wiley, New York, 1989).
8. D. M. Driscoll, J. K. Wynne, S. C. Wallis, J. Scott, *Cell* **58**, 519 (1989); J. H. Wu, C. F. Semenkovich, S. H. Chen, W. H. Li, L. Chan, *J. Biol. Chem.* **265**, 12312 (1990). Nuclear and S100 extracts were prepared as in (7). The standard in vitro assay (20 μl) contained 50 fmol of RNA substrate, 50 μg of nuclear or S100 extract protein, 10 mM Hepes (pH 7.9), 10% glycerol, 50 mM KCl, 50 mM EDTA, and 0.25 mM dithiothreitol. The reactions were incubated at 30°C for 3 hours.
9. For synthesis of the in vitro RNA substrate, a 646-bp DNA fragment corresponding to positions −256 to +390 was cloned into the transcription vector pBKSII$^-$ (Stratagene) and linearized with Bam HI. RNA labeled with [α-^{32}P]uridine 5′-triphosphate (UTP) was transcribed (specific activity = 2.2 x 10^6 cpm/mmol) with T3 RNA polymerase. The reaction was treated with 10 U of ribonuclease-free deoxyribonuclease (Promega) at 37°C for 40 min, extracted with phenol-chloroform (1:1), and precipitated with ethanol.
10. In vitro products were amplified by RS-PCR [A. R. Shuldiner, R. Perfetti, J. Roth, in *PCR Protocols: Current Methods and Applications*, B. A. White, Ed. (Humana, Totowa, NJ, 1993), pp. 169–176]. The cDNA was synthesized with an antisense oligonucleotide containing a 5′-terminal extension (5′-AATCCGGATTGCCCGGAACGTCTTGGCGAAATATCGCATCCTTGC-3′). The cDNA products were selectively amplified with an antisense PCR primer unique to the RNA-derived cDNA extension sequence. Hybridization and extension of a [γ-^{32}P]-labeled 15-nt oligomer sense primer (−18 to −4) in the presence of dideoxy-ATP generated products of 19 and 22 nt for nonedited and edited transcripts, respectively.
11. Protease sensitivity and thermolability studies were performed by preincubation of HeLa cell nuclear extracts (50 μg) with 1 μg of proteinase K for 20 min at 37°C or by preincubation at elevated temperature (65°C and 85°C) for 10 min, respectively. Micrococcal nuclease sensitivity was determined by pretreatment of extracts with $CaCl_2$ (0.75 mM final concentration) and 13.5 U of micrococcal nuclease (Pharmacia) for 10 min at room temperature. Micrococcal nuclease was inactivated by the addition of EGTA (2.5 mM final concentration).
12. Construction of mutant GluR-B RNA substrates was performed by oligonucleotide-directed mutagenesis in pBKSII$^-$ (Stratagene) as previously described (7).
13. In competition studies, cDNA was synthesized with an oligonucleotide complementary to the pRC/CMV-derived 3′ extension of the GluR-B RNA substrate. The ssDNA competitor (81 nt) was an oligonucleotide derived from the neomycin resistance gene (pRC/CMV); the dsDNA competitor (178 bp) was obtained by PCR amplification of pBKSII$^-$ polylinker. The ssRNA competitors were transcribed in the presence of [α-^{32}P]UTP (specific activity = 2.2 x 10^6 cpm/mmol) from pBKSII$^-$ linearized with Xba I (93 nt) or Xho I (97 nt). The dsRNA competitor was produced by annealing the ssRNAs in 80% formamide, 40 mM Pipes (pH 6.4), 400 mM NaCl, and .1.25 mM EDTA for 14 to 16 hours at 25°C. Residual ssRNA was removed by ribonuclease A digestion (25 μg/ml) (7). The dsRNA was purified on an 8% nondenaturing acrylamide gel and eluted by incubation in 1 M ammonium acetate, 10 mM tris-HCl (pH 7.6), and 1 mM EDTA for 2 hours at 4°C.
14. B. L. Bass and H. Weintraub, *Cell* **48**, 607 (1987); R. W. Wagner and K. Nishikura, *Mol. Cell. Biol.* **8**, 770 (1988); U. Kim and K. Nishikura, *Semin. Cell. Biol.* **4**, 285 (1993).
15. The 646-nt RNA substrate was transcribed in the presence of [α-^{32}P]ATP (800 Ci/mmol) or [2,8-^{3}H]ATP (30 Ci/mmol) (RNA specific activity, 4.9 x 10^{10} and 9.6 x 10^9 cpm/mmol, respectively). After the standard in vitro reaction, one-half of the product was used to quantitate GluR-B RNA editing by the RS-PCR primer extension assay, and the remainder of the reaction was resuspended in 50 mM sodium acetate (pH 5.3), digested with nuclease P1 at 37°C for 2 hours, and spotted onto a cellulose TLC plate (Sigmacell Type 100). Chromatography proceeded for ~6 hours in 0.1 M NaH_2PO_4 (pH 6.8), ammonium sulfate, and *n*-propanol (100:60:2, v/w/v) as described (16). The migration positions of nucleoside monophosphate standards were determined by ultraviolet light absorption, and the migration positions of the [^{32}P]-labeled products were detected by autoradiography and quantitated with a Molecular Dynamics phosphorimager. For detection of [^{3}H]-labeled reaction products, 0.5-cm cellulose fractions from the TLC plate were counted by liquid scintillation spectrometry.
16. M. Silberklang, A. M. Gillum, U. L. RajBhandary, *Methods Enzymol.* **59**, 58 (1979).
17. G. A. Garcia, K. A. Koch, S. Chong, *J. Mol. Biol.* **231**, 489 (1993); M. S. Elliott and R. W. Trewyn, *J. Biol. Chem.* **259**, 2407 (1984).
18. A. G. Polson and B. L. Bass, *EMBO J.* **13**, 5701 (1994).

19. We thank J. Lu, J. Patton, R. Breyer, and B. Wadzinski for critical reading of the manuscript and J. Patton for providing HeLa cell extracts. Supported by grants from the National Parkinson Foundation and NIH (ES00267).

30 December 1994; accepted 9 February 1995

Involvement of CRAF1, a Relative of TRAF, in CD40 Signaling

Genhong Cheng,* Aileen M. Cleary,* Zheng-sheng Ye,* David I. Hong, Seth Lederman, David Baltimore†

CD40 is a receptor on the surface of B lymphocytes, the activation of which leads to B cell survival, growth, and differentiation. A yeast two-hybrid screen identified a gene, *CRAF1*, encoding a protein that interacts directly with the CD40 cytoplasmic tail through a region of similarity to the tumor necrosis factor–α (TNF-α) receptor–associated factors. Overexpression of a truncated *CRAF1* gene inhibited CD40-mediated up-regulation of CD23. A region of *CRAF1* was similar to the TNF-α receptor–associated factors TRAF1 and TRAF2 and so defined a shared TRAF-C domain that was necessary and sufficient for CD40 binding and homodimerization. The CRAF1 sequence also predicted a long amphipathic helix, a pattern of five zinc fingers, and a zinc ring finger. It is likely that other members of the TNF receptor superfamily use *CRAF*-related proteins in their signal transduction processes.

CD40 (*1*) is a receptor on B cells that interacts with the helper T cell surface protein CD40L (CD40 ligand, also known as T-BAM, gp39, or TRAP) (*2–4*). CD40L is found particularly on lymphoid follicle CD4$^+$ T lymphocytes, where it delivers a contact-dependent signal that stimulates B cell survival, growth, and differentiation (*2–4*). Signaling through CD40 rescues B cells from apoptosis induced by Fas (CD95) or by cross-linking of the immunoglobulin M (IgM) complex (*5*); it also induces B cells to differentiate and to undergo Ig isotype switching (*3*) and to express CD80 (B7 or BB-1) (*6*). The crucial role of CD40L-CD40 interaction is illustrated by humans with defects in CD40L, who manifest a serious immune deficiency syndrome, the X-linked hyper-IgM syndrome (HIGMX-1), characterized by an absence of IgG, IgA, and IgE, elevated IgM, and no lymphoid

G. Cheng and D. Baltimore, Department of Biology, Massachusetts Institute of Technology, 77 Massachusetts Avenue, Cambridge, MA 02139, USA.
A. M. Cleary, D. I. Hong, S. Lederman, Department of Medicine, Columbia University, New York, NY 10032, USA.
Z.-s. Ye, Rockefeller University, 1230 York Avenue, New York, NY 10021, USA.

*These authors contributed equally to this work.
†To whom correspondence should be addressed.

follicles (*7*). The essential roles of CD40L and CD40 in the phenotype of HIGMX-1 syndrome has been confirmed by targeted disruption of either CD40L (*8*) or CD40 (*9*) in mice. In addition to B cells, CD40 is also expressed by follicular dendritic cells (*10*), dendritic cells (*11*), activated macrophages (*12*), epithelial cells (including thymic epithelium) (*13*), and a variety of tumor cells.

Stimulation of CD40 causes the tyrosine phosphorylation of multiple substrates including Src family kinases such as p53-p56^{lyn}, activates multiple serine-threonine–specific protein kinases, and induces the phosphorylation of phospholipase C-γ2 and of phosphoinositide-3′ kinase (*14*). The initial stage of signaling by CD40, however, is not yet characterized. Because the murine CD40 cytoplasmic tail is necessary for signaling (*15*), we have used the yeast two-hybrid system in an effort to identify complementary DNAs (cDNAs) encoding protein domains that can bind to the tail (*16*). From 2 × 10^6 clones of a murine 70Z pre-B cell cDNA library (*17*), one (C26) was isolated that met all specificity criteria for binding to the cytoplasmic tail of CD40 in yeast. The C26 cDNA fragment was sequenced and no identical gene was evident in the databases. We call this gene *CRAF1* for CD40 receptor–associated factor 1. By Northern (RNA) blot analysis, *CRAF1* was expressed in B cell lines representing different stages of B cell differentiation; in addition, it was expressed in all murine tissues examined, including brain, heart, lung, liver, kidney, muscle, small intestine, spleen, and thymus (*18*). Thus, it may well serve functions in other pathways.

Mouse and human cDNA libraries were screened to isolate cDNA clones encoding the entire open reading frame of a murine 567–amino acid and a human 568–amino acid protein. The two sequences share 96% identity, with the differences concentrated near the NH_2-terminus, indicating that *CRAF1* is evolutionarily conserved, particularly in its COOH-terminal 400 amino acids (Fig. 1). The CRAF1 sequence is similar to that of TNF-α receptor–associated factors 1 and 2 (TRAF1 and TRAF2), which can complex with the cytoplasmic tail of TNF-α receptor II (TNFαRII) (*19*). The COOH-terminus of CRAF1 is related by sequence to each of these TRAF proteins for 150 amino acids, wherein CRAF1 is 59 and 62% identical to TRAF1 or TRAF2, respectively (Fig. 2) (*19*). This homology subdivides what was termed the "TRAF domain," excluding a more NH_2-terminal putative coiled-coiled subdomain (TRAF-N) with which CRAF1 shares only 16 or 12% homology and defines a "TRAF-C" (for COOH-terminal) domain. Because the extracellular domains of CD40 and TNFαRII are homologous, as are their ligands, these data suggest that they may make use of related but distinct signaling molecules. However, the cytoplasmic domains of CD40 and TNFαRII contain no apparent sequence homology, which suggests that the particular contacts involved in binding the signaling molecules to the receptors have diverged.

In addition to the TRAF-C domain, sequence analysis of the CRAF1 protein revealed three potential domains: an amphipathic helix, a string of Zn fingers, and a Zn ring finger domain (Fig. 2A). A helical wheel representation of the putative helix (Fig. 2B) shows that isoleucine (or occasionally leucine) repeats every seven residues through eight consecutive repeats, which implies the presence of a isoleucine zipper in analogy to the leucine zipper seen in other

Fig. 1. Predicted amino acid sequences of mouse (M) and human (H) CRAF1 (*22*). The full-length mouse sequence is shown and numbered. The human sequence has one more amino acid than that of the mouse (indicated with a dot), but all numbers here refer to the mouse sequence. Dashes indicate positions in the human sequence that are identical to those in the mouse. The C26 clone obtained from the yeast two-hybrid screen contained the COOH-terminal region of CRAF1 starting from the position marked with an arrow. The cDNA nucleotide sequences are deposited in GenBank with accession numbers U21050 and U21092.

```
M  MESSKKMDAAGTLQPNPPLKLQPDRGAG.SVLVPEQGGYKEKFVKTVEDK   49
H  --------SP-A--T------HT--S--TP-F------------------

M  YKCEKCRLVLCNPKQTECGHRFCESCMAALLSSSSPKCTACQESIIKDKV   99
H  ------H----S--------------------------------V----

M  FKDNCCKREILALQVYCRNEGRGCAEQLTLGHLLVHLKNECQFEELPCLR  149
H  -------------I-----S-----------------D-H------V-

M  ADCKEKVLRKDLRDHVEKACKYREATCSHCKSQVPMIKLQKHEDTDCPCV  199
H  P-----------------------------------A------------

M  VVSCPHKCSVQTLLRSELSAHLSECVNAPSTCSFKRYGCVFQGTNQQIKA  249
H  ---------------------------------------------------

M  HEASSAVQHVNLLKEWSNSLEKKVSLLQNESVEKNKSIQSLHNQICSFEI  299
H  ---------------------------------------------------

M  EIERQKEMLRNNESKILHLQRVIDSQAEKLKELDKEIRPFRQNWEEADSM  349
H  ---------------------------------------------------

M  KSSVESLQNRVTELESVDKSAGQAARNTGLLESQLSRHDQTLSVHDIRLA  399
H  ----------------------V----------------M---------

M  DMDLRFQVLETASYNGVLIWKIRDYKRRKQEAVMGKTLSLYSQPFYTGYF  449
H  ---------------------------------------------------

M  GYKMCARVYLNGDGMGKGTHLSLFFVIMRGEYDALLPWPFKQKVTLMLMD  499
H  ---------------------------------------------------

M  QGSSRRHLGDAFKPDPNSSSFKKPTGEMNIASGCPVFVAQTVLENGTYIK  549
H  ---------------------------------------------------

M  DDTIFIKVIVDTSDLPDP                                   567
H  ------------------
```

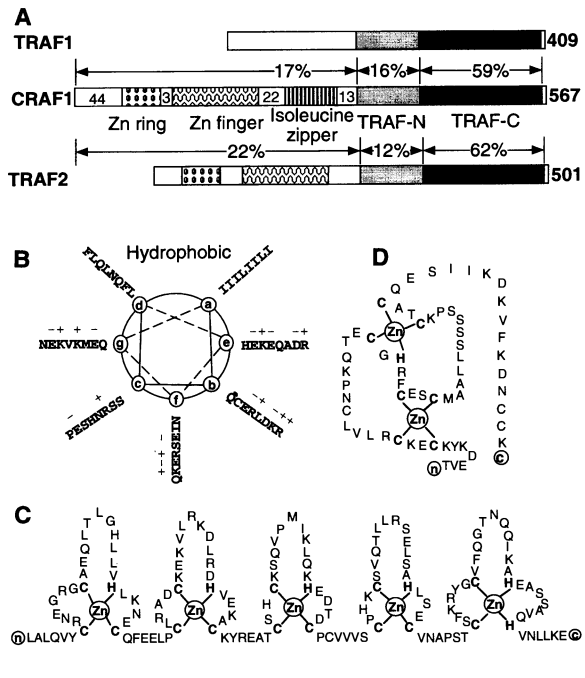

Fig. 2. Potential structural domains of CRAF1 (*22*). (**A**) Diagrams of three TRAF family members. Percentages of amino acid identity between CRAF1 and either TRAF1 or TRAF2 are shown. The TRAF domain was defined in the COOH-terminal region of TRAF1 and TRAF2 (*19*) (residues 356 to 562 for CRAF1) but can be subdivided into TRAF-N and TRAF-C subregions according to sequence homology with CRAF1 as well as by the mapping assays shown in Fig. 3. For CRAF1, the number of amino acids between homologous regions is indicated. (**B**) Helical wheel representation of residues 287 to 342 of CRAF1. The wheel starts with the inner residue Ile^{287} at position a and finishes with the outer residue Asn^{342} at position g; "+" and "−" denote change of amino acid residues. (**C**) Predicted Zn fingers corresponding to residues 110 to 264 of CRAF1. (**D**) Zn finger from residues 45 to 106 of CRAF1. n, NH_2-terminus; c, COOH-terminus.

proteins (*20*). The wheel also indicates that the position next to the zipper is always hydrophobic or uncharged, whereas the other positions around the wheel include multiple charged residues and few hydrophobic ones. This strongly suggests an amphipathic structure that could be an interaction site for another such helix.

There are five repeats of potential Zn fingers just NH_2-terminal to the isoleucine repeats (Fig. 2C). However, the four amino acids that would contact the metal are arranged in the unique pattern Cys-X_{2-6}-Cys-$X_{11,12}$-His-X_{3-7}-Cys(His), instead of Cys-X_{2-4}-Cys-$X_{12,13}$-His-X_{2-4}-His, which is seen in classic Zn fingers (*21*). At the COOH-terminal edge of finger 2 is a sequence (KACKYR) (*22*) that could bind to DNA, which suggests that CRAF1 might be a DNA binding protein. In the TRAF2 protein, we found five fingers with the same pattern of repeats seen in the CRAF1 protein but with weak overall similarity (Fig. 2A), suggesting that these structural units may represent a subclass of Zn finger motifs in this type of signaling molecule. In addition, a Zn ring structure was also evident in the NH_2-terminus of CRAF1 (Fig. 2D) (*23*). This ring motif has been recognized in over 40 proteins that have diverse functions related to DNA mechanics, including recombination, repair, and transcription regulation (*24*). These structural data suggest that CRAF1 could directly transmit CD40 signals to the nucleus.

To further map the region of CRAF1 that interacts with the CD40 cytoplasmic tail, we generated four deletion mutants of the C26 cDNA and studied them in the yeast system for their ability to bind to the CD40 cytoplasmic tail. The TRAF-C subdomain of CRAF1 was necessary and sufficient for CRAF1 to interact with CD40 (Fig. 3). Moreover, the CRAF1 protein in yeast could interact with itself, forming homodimers or oligomers, also mediated by the TRAF-C domain (Fig. 3). Quantitative analysis of β-galactosidase expression indicated that the affinity of the TRAF-C domain of CRAF1 to bind to CD40 and to dimerize with itself was not increased by addition of the rest of the TRAF domain. We therefore suggest that the COOH-terminal portion of the TRAF domain may function as an individual unit (the TRAF-C domain) that is involved in both binding to the receptor tail and mediating dimerization.

To determine if the CD40-binding domain of CRAF1 can play a functional role in mammalian cells, we examined whether overexpression of the C26 partial cDNA fragment would act as a dominant negative protein, inhibiting CD40 signaling presumably by prevention of the binding of the endogenous protein to the CD40 tail. Ramos 2G6 cells (*25*) can be induced to up-regulate

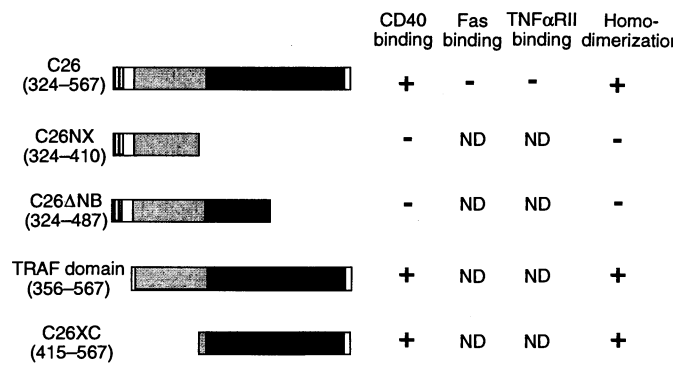

Fig. 3. Mapping the CD40 binding and homodimerization domain of CRAF1. C26NX and C26XC represents fragments from the NH_2-terminus of C26 to the internal Xho I site and from the Xho I site to the COOH-terminus of CRAF1, respectively. C26ΔNB was made by deletion of the Nco I–Bgl II fragment in the 3′ untranslated region of the C26 cDNA clone. The full TRAF domain of CRAF1 was synthesized by the polymerase chain reaction with the use of plaque-forming units of DNA polymerase. Various DNA fragments were ligated in-frame into yeast expression vectors encoding either the LexA DNA-binding domain (LexA) or the transcriptional activation domain (TAD). For CD40 binding assays, the LexA construct containing the CD40 cytoplasmic tail and various TAD fusion constructs were cotransfected into yeast strain EGY48 along with the lacZ-containing reporter vector (pSH18-34). Colonies that grew up on synthetic dextrose plates without tryptophan, uracil, and histidine were replica-plated to plates with or without leucine and tested for galactose-inducible blue color in the presence of x-gal. LexA constructs containing the cytoplasmic tails of Fas and TNFαRII were also included in the same experiments to test their interaction with the C26 clone. For dimerization assays, various LexA fusion constructs containing different fragments of C26 were used in every combination with various TAD fusion constructs. Transformants that grew on plates lacking leucine and that showed galactose-inducible blue are marked "+"; this was further confirmed by β-galactosidase assays with the use of yeast grown in liquid cultures (*34*). Transformants that grew only on plates containing leucine but that did not show blue on x-gal plates are marked "−"; ND, experiments not done.

surface CD23 molecules in a contact-dependent fashion that depends on CD40L interaction with CD40 (*3*). Therefore, a cDNA construct was generated that drives the expression of a polyhistidine/C26 fusion protein (pEBVHis/C26) in mammalian cells (*26*). As a negative control for the effects of C26, the β-galactosidase gene was expressed as a fusion protein in the same vector (pEBVHis/lacZ) (Invitrogen). These constructs were electroporated into Ramos 2G6 cells, and clones expressing a large amount of pEBVHis/C26 mRNA were prepared (Fig. 4A). CD40L-expressing cells (293.CD40L) were then cultured with Ramos 2G6 cells that either were not transfected or were stably expressing pEBVHis/lacZ or pEBVHis/C26 (*27*). The control and pEBVHis/lacZ-transfected Ramos lines up-regulated CD23; this effect was inhibited by a monoclonal antibody (mAb) to CD40L (mAb 5C8). In contrast, the ability of the pEBVHis/C26 transfectants to up-regulate CD23 in response to CD40L-CD40 signals was diminished. The inhibition of CD23 up-regulation by pEBVHis/C26 was relatively specific because recombinant interleukin-4 (rIL-4)–induced up-regulation of CD23 was not affected (Fig. 4B). Similar effects were seen in all three subclones of pEBVHis/C26 transfectants. Thus, the COOH-terminal region of CRAF1 represented in the C26 cDNA could block the CD40 triggering of Ramos cells, suggesting that CRAF1 participates in CD40 signaling.

CD40 is a type I transmembrane glycoprotein belonging to the TNF receptor superfamily. Besides CD40, 11 other proteins have been identified in this superfamily, which includes TNF receptors I and II, the nerve growth factor (NGF) receptor, and Fas (*28*). Members within this family share sequence similarity through their extracellular regions that contain multiple cysteine-rich pseudorepeats. The common structural framework of the extracellular domain is reflected in the ability of the TNF receptor superfamily members to interact with a parallel family of TNF-related cytokine ligands. To date, eight such ligands (including TNF-α, CD40L, and FasL) have been cloned that share extensive sequence identity and exist as secreted cytokines or type II transmembrane ligands (*28*).

The functions of TNF receptor superfamily members are very divergent. They range from general acute phase responses and lymphocyte activation to nerve cell growth. In some circumstances, they have opposite roles. For instance, Fas and TNFαRI can cause apoptosis upon ligand stimulation, whereas CD40 and NGF receptors can rescue cells from apoptosis (*29*). In addition, stimulation of either TNFαRI, TNFαRII, or CD40 receptor activates nuclear factor kappa B (*30*). Because CRAF1 is very similar to TRAF1 and TRAF2, a family of signal transduction proteins (the TRAF family) probably exists as downstream signal transducers of the TNF receptor superfamily. It is likely that direct binding between members of the TNF receptor family and the TRAF family will be specific because the cytoplasmic tails of these TNF receptor superfamily members are relatively short and show little or no sequence homology. Consistent with this

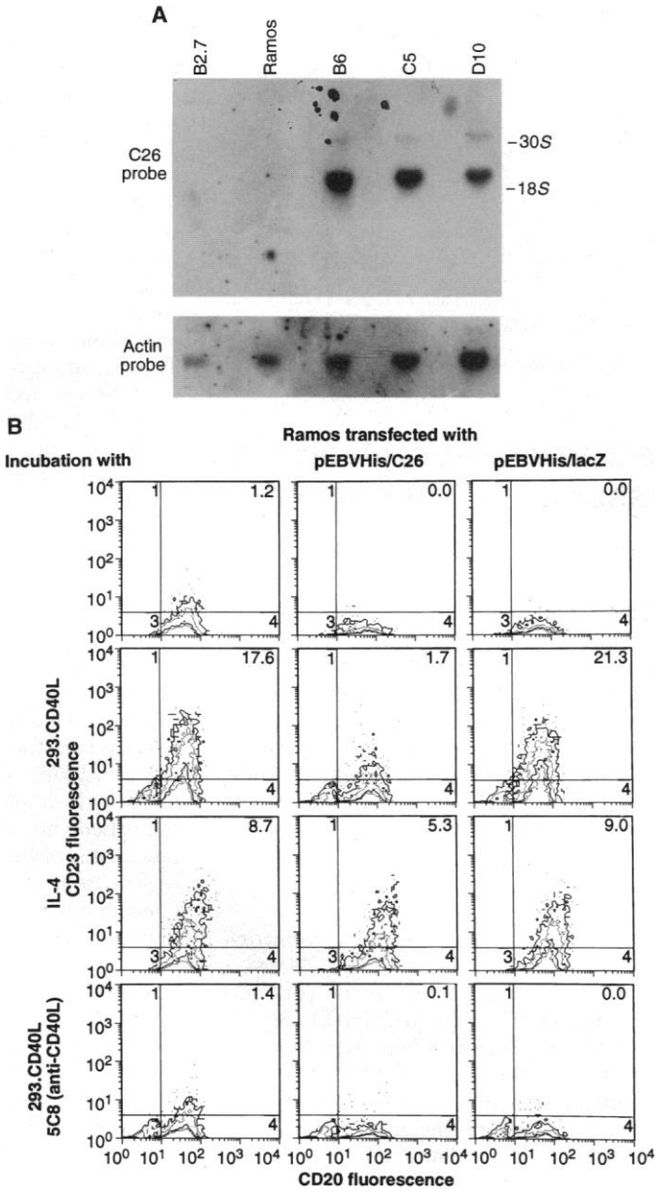

Fig. 4. Effect of C26 fusion proteins on CD40L: CD40–induced CD23 up-regulation. (**A**) Northern blot analysis of Ramos 2G6 transfectants. Total RNA (2 μg) from the Jurkat T cell line (B2.7) was used for markers. In other lanes, polyadenylate-containing RNA (0.75 μg per lane) was obtained from the untransfected Ramos 2G6 clone (Ramos) or pEBVHis/C26 Ramos transfectants (B6, C5, or D10). RNA blots of control and transfected cell lines were probed with C26 cDNA or an actin probe. (**B**) Two-color fluorescence-activated cell sorting analysis of Ramos 2G6 and Ramos 2G6 transfectants (pEBVHis/C26 or pEBVHis/lacZ) after 18 to 24 hours of culture with medium (−), 293.CD40L cells, rIL-4, or 293.CD40 cells plus anti-CD40L mAb 5C8 (as indicated). The *x* and *y* axes represent CD20 and CD23 fluorescence, respectively. The percentage of $CD20^+$ cells that express CD23 is indicated in the upper right-hand corner of each contour map. The D10 clone of pEBVHis/C26 is shown.

notion, we found that the COOH-terminal segment of CRAF1 does not interact with the tail of Fas or with TNFαRII (Fig. 3). However, the fact that the members of the TRAF family can form either homodimers or heterodimers could result in extensive diversity and specificity in their signal transduction pathways. It is even possible that apoptosis and cell survival may be determined by an equilibrium of dimerization between TRAF family members.

The functional consequences of CD40 signaling are different for B cells at different stages of differentiation (*31*). CD40 crosslinking causes resting B cells to enter into the cell cycle, enhances the proliferative rate of some chronic lymphocytic leukemia B cells, induces some B lymphoma cells to apoptose, and prevents germinal center B cells from apoptosis (*14*). However, CRAF1 is expressed at all stages of B cell differentiation and may be ubiquitous. It could have more specific partners or specifity may be a result of how a common signal is interpreted in a given cell.

Note added in proof: After submission of our paper, Hu *et al.* (*32*) and Mosialos *et al.* (*33*) described proteins that interact with the cytoplasmic tail of CD40. Their proteins are identical to CRAF1.

REFERENCES AND NOTES

1. S. Paulie *et al.*, *Cancer Immunol. Immunother.* **20**, 23 (1985); E. A. Clark and J. A. Ledbetter, *Proc. Natl. Acad. Sci. U.S.A.* **83**, 4494 (1986); I. Stamenkovic, E. A. Clark, B. Seed, *EMBO J.* **8**, 1403 (1989).
2. S. Lederman *et al.*, *J. Exp. Med.* **175**, 1091 (1992); R. J. Armitage *et al.*, *Nature* **357**, 80 (1992); D. Graf, U. Korthauer, H. W. Mages, G. Senger, R. A. Kroczek, *Eur. J. Immunol.* **22**, 3191 (1992); J. F. Gauchat *et al.*, *FEBS Lett.* **315**, 259 (1993).
3. S. Lederman *et al.*, *J. Immunol.* **149**, 3817 (1992).
4. D. Hollenbaugh *et al.*, *EMBO J.* **11**, 4313 (1992).
5. T. Tsubata, J. Wu, T. Honjo, *Nature* **364**, 645 (1993); N. J. Holder *et al.*, *Eur. J. Immunol.* **23**, 2368 (1993); S. L. Parry, J. Hasbold, M. Holman, G. G. B. Klaus *J. Immunol.* **152**, 2821 (1994); A. M. Cleary, S. M. Fortune, L. Chess, S. Lederman, unpublished results.
6. M. J. Yellin *et al.*, *J. Immunol.* **153**, 666 (1994).
7. R. C. Allen *et al.*, *Science* **259**, 990 (1993); U. Korthäuer *et al.*, *Nature* **361**, 539 (1993); J. P. DiSanto *et al.*, *ibid.*, p. 541; A. Aruffo *et al.*, *Cell* **72**, 291 (1993); R. E. Callard *et al.*, *J. Immunol.* **153**, 3295 (1994); N. Ramesh *et al.*, *Int. Immunol.* **5**, 769 (1993).
8. J. Xu *et al.*, *Immunity* **1**, 423 (1994).
9. T. Kawabe *et al.*, *ibid.*, p. 167.
10. F. Schrieve *et al.*, *J. Exp. Med.* **169**, 2043 (1989); E. A. Clark, K. H. Grabstein, G. L. Shu, *J. Immunol.* **148**, 3327 (1992).
11. D. N. Hart and J. L. McKenzie, *J. Exp. Med.* **168**, 157 (1988).
12. M. R. Alderson *et al.*, *ibid.* **178**, 669 (1993).
13. A. H. Galy and H. Spits, *J. Immunol.* **149**, 775 (1992).
14. F. H. Durie, T. M. Foy, S. R. Masters, J. D. Laman, R. J. Noelle, *Immunol. Today* **15**, 406 (1994).
15. S. Inui *et al.*, *Eur. J. Immunol.* **20**, 1747 (1990).
16. The bait for the yeast two-hybrid screen was a LexA fusion protein containing the cytoplasmic tail of the mouse CD40 receptor (from residue 219 to the COOH-terminus).
17. The cDNA library for the yeast two-hybrid screen was a mixture of oligo(dT) and random primed cDNAs constructed into the yeast expression vector YSD, which is a centromere-based, galactose-induced yeast expression vector containing the VP16 transcription activation domain. Half of the mRNA used for cDNA synthesis was isolated from uninduced 70Z cells, and the other half was from 70Z cells that were induced with lipopolysaccharide for 12 hours. The primary library contained about 8×10^5 individual clones, with an average insert size of 0.9 kb.
18. G. Cheng, Z. S. Ye, D. Baltimore, unpublished results.
19. M. Rothe, S. C. Wong, W. J. Henzel, D. V. Goeddel, *Cell* **78**, 681 (1994).
20. W. H. Landschulz, P. F. Johnson, S. L. McKnight, *Science* **240**, 1759 (1988).
21. R. M. Evans and S. M. Hollenberg, *Cell* **52**, 1 (1988).
22. Abbreviations for the amino acid residues are A, Ala; C, Cys; D, Asp; E, Glu; F, Phe; G, Gly; H, His; I, Ile; K, Lys; L, Leu; M, Met; N, Asn; P, Pro; Q, Gln; R, Arg; S, Ser; T, Thr; V, Val; W, Trp; and Y, Tyr.
23. P. S. Fremont, I. M. Hanson, J. Trowsdale, *ibid.* **64**, 483 (1991).
24. P. N. Barlow, B. Luisi, A. Milner, M. Elliott, R. Everett, *J. Mol. Biol.* **237**, 201 (1994).
25. J. P. Siegel and H. S. Mostowski, *J. Immunol. Methods* **132**, 287 (1990).
26. The C26 cDNA fragment was cut with Eco RI–Hinc III from yeast vector YSD, ligated into Bluescript IISK+ (Stratagene), and then recloned in-frame into the pEBVHisA vector (Invitrogen), with the use of Bam HI and Kpn I cuts, to create pEBVHis/C26. Stable Ramos cell lines containing either this construct or the control construct (pEBVHis/lacZ) were isolated by electroporation and hygromycin selection.
27. Either 2×10^5 Ramos B cells or Ramos B cells transfected with pEBVHis/C26 or pEBVHis/lacZ were incubated for 18 to 24 hours in 0.2 ml of medium alone, in rIL-4 at a concentration of 25 ng/ml, or in the presence of 5×10^4 293.CD40L cells. In some cases, mAb 5C8 (anti-CD40L) was added. Cells were then washed and incubated with saturating concentrations of mAb Leu-16 (anti-CD20) conjugated to fluorescein isothiocyanate (Becton Dickinson) and mAb to CD23 conjugated to phycoerythrin (Biosource International) for 45 min at 4°C in the presence of heat-aggregated IgG (80 μg/ml) (International Enzyme). Cells were washed to remove unbound antibody before fluorescence intensity was measured on a FACSCAN cytofluorograph (Becton Dickinson) with Consort 30 software.
28. C. A. Smith, T. Farrah, R. G. Goodwin, *Cell* **76**, 959 (1994).
29. N. Itoh *et al.*, *ibid.* **66**, 233 (1991); L. A. Taraglis, T. M.

Ayres, G. H. W. Wong, D. V. Goeddel, *ibid.* **74**, 845 (1993).
30. M. Grilli, J. J.-S. Chiu, M. J. Lenardo, *Int. Rev. Cytol.* **143**, 1 (1991); I. Berberich, G. L. Shu, E. A. Clark, *J. Immunol.* **153**, 4357 (1994).
31. J. Gordon, M. J. Millsum, G. R. Guy, J. A. Ledbetter, *J. Immunol.* **140**, 1425 (1988); M. F. Gruber, J. M. Bjorndahl, S. Nakamuar, S. M. Fu, *ibid.* **142**, 4144 (1989); M. K. Spriggs *et al.*, *J. Exp. Med.* **176**, 1543 (1992); P. Lane *et al.*, *ibid.* **177**, 1209 (1993); D. H. Crawford and D. Catovsky, *Immunology* **80**, 40 (1993); A. W. Heath *et al.*, *Cell Immunol.* **152**, 468 (1993); Y.-J. Liu *et al.*, *Nature* **342**, 929 (1989).
32. H. M. Hu, K. O'Rourke, M. S. Boguski, V. M. Dixit, *J. Biol. Chem.* **269**, 30069 (1994).
33. G. Mosialos *et al.*, *Cell* **80**, 389 (1995).
34. J. H. Miller, in *Experiments in Molecular Genetics*, C. S. H. L. Press, Ed. (Cold Spring Harbor Laboratory, Cold Spring Harbor, NY, 1972).
35. We thank P. Svec and T. Hawkins for their help in sequencing and J. Jacob for critical reading of the manuscript. G.C. and Z.-Y. are recipients of an Irvington House Institute fellowship and a Leukemia Society special fellowship, respectively. S.L. is an Arthritis Investigator of the Arthritis Foundation. D.B. is an American Cancer Society Research Professor. A.M.C. is supported by the Medical Scientist Training Program grant 5-T32-GM07367. S.L., A.M.C., and D.I.H. are also supported in part by Biogen, Cambridge, MA. This work was supported by National Institute of Allergy and Infectious Diseases grant A122346 (D.B.) and by National Cancer Institute (NCI) grant R01-CA55713 to S.L.

22 November 1994; accepted 2 February 1995

Crystal Structure of the Tetramerization Domain of the p53 Tumor Suppressor at 1.7 Angstroms

Philip D. Jeffrey, Svetlana Gorina, Nikola P. Pavletich

The p53 protein is a tetrameric transcription factor that plays a central role in the prevention of neoplastic transformation. Oligomerization appears to be essential for the tumor suppressing activity of p53 because oligomerization-deficient p53 mutants cannot suppress the growth of carcinoma cell lines. The crystal structure of the tetramerization domain of p53 (residues 325 to 356) was determined at 1.7 angstrom resolution and refined to a crystallographic *R* factor of 19.2 percent. The monomer, which consists of a β strand and an α helix, associates with a second monomer across an antiparallel β sheet and an antiparallel helix-helix interface to form a dimer. Two of these dimers associate across a second and distinct parallel helix-helix interface to form the tetramer.

The p53 tumor suppressor (*1*), a tetrameric protein that can bind to specific DNA sequences (*2*) and activate gene expression (*3*, *4*), plays a central role in a cell's response to tumorigenic events. p53 can induce cell cycle arrest in response to DNA damage and thus can prevent genetic alterations such as chromosomal rearrangements and gene amplifications (*5*). In addition to coordinating the DNA damage response, p53 can also induce apoptosis in response to the activation of oncogenes such as c-Myc and E1A (*6*). These findings suggest that p53 exerts its tumor suppressing effects by responding to events that may lead to the abnormal proliferation of cells.

The p53 protein has multiple domains with the DNA binding, transactivation, and tetramerization functions residing in separate domains. The sequence-specific DNA binding activity resides in the central portion which folds into a compact structural domain [core domain, residues 102 to 292 (*7*–*9*)]; the transactivation function resides in the loosely folded NH_2-terminal portion [residues 1 to 44 (*3*, *7*)]; and the tetramerization function resides in a structural domain in the COOH-terminal portion of the protein [residues 320 to 356 (*7*, *9*–*11*)]. Consistent with its tetrameric oligomerization state, the p53 protein binds DNA sites that contain four repeats of the pentamer sequence motif Pu-Pu-Pu-C-(A/T) (*2*).

DNA binding and transactivation are the critical mediators of p53's biological effects because tumor-derived p53 mutants defective in suppressing growth are also defective in DNA binding and transactivation (*3*). In vitro, tetramerization is not essential for DNA binding, and the isolated core domain can bind DNA with approximately one-fifth the affinity of intact p53 (*7*). In vivo, however, oligomerization-deficient p53 cannot efficiently transactivate from genomic p53 binding sites in transient transfection assays (*12*), and it cannot suppress the growth of carcinoma cell lines (*12*, *13*). This suggests that there is a tight threshold for in vivo p53 activity and that oligomerization is required to maintain this activity above threshold (*12*). These findings are analogous to those obtained with several tumorigenic mutants of p53 which bind to DNA with reduced affinity but fail to suppress growth in vivo (*14*).

Using a peptide that corresponds to residues 320 to 356 of p53 (*15*), we have obtained three crystal forms of the tetramer and have determined the structure by the multiple isomorphous replacement method (MIR) (*15*). The quaternary structures in the three crystal forms are essentially identical; therefore, our discussion of the tetramer structure will focus on the tetragonal crystal form that diffracts to beyond 1.7 Å resolution and has been refined to a crystallographic *R* factor of 19.2% (Table 1 and Fig. 1).

The crystal structure of the tetramer reveals that the oligomerization domain contains a β strand from residue 326 to 333 and an α helix from residue 335 to 354. The β strand and the α helix form a V-shaped structure with the helix axis being roughly antiparallel to the direction of the β strand. The transition from the β strand to the α helix occurs over a single residue, Gly^{334}, with the backbone amide nitrogen of the glycine making the last β sheet hydrogen bond and the backbone carbonyl making the first α helical hydrogen bond. The backbone conformation ($\phi = 98°$, $\psi = 130°$) in this hinge region is unique to the glycine amino acid, and it is energetically unfavorable for other amino acids. Consistent with its role as a critical hinge residue between the β strand and the α helix, Gly^{334} is conserved across species (*16*) and is one of the few oligomerization domain residues that has been found to be mutated in tumors (*17*). Flanking the Gly^{334} hinge region, there are hydrophobic interactions between the α helix and the β strand involving the side chains of Ile^{332}, Phe^{338}, and Phe^{341}.

The tetramer has 222-point symmetry (three mutually perpendicular twofold rotation axes), with each of the four monomers being in an identical environment (Fig. 2). The tetragonal crystal form has one monomer in the asymmetric unit, and the three twofold symmetry axes of the tetramer coincide with crystallographic symmetry. The twofold axes intersect at the center of the tetramer near the side chain of Leu^{344}. In the

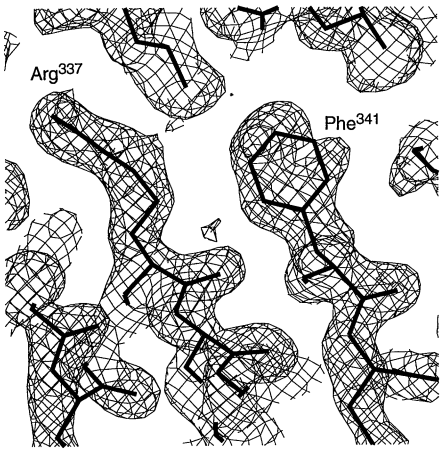

Fig. 1. Multiple isomorphous replacement (MIR) electron density map calculated with phases from the program SQUASH (*34*) at 2.0 Å and contoured at 1.0σ. The Arg^{337} and Phe^{341} residues are labeled. The helix axis is approximately horizontal in the figure.

Cellular Biochemistry and Biophysics Program, Memorial Sloan-Kettering Cancer Center, New York, NY 10021, USA.